

Synthesis of Anisotropic Gold Nanoparticles by Electrospraying into a Reductive-Surfactant Solution

Asuncion Quintanilla,^{*,†} Mario Valyo,[‡] Ugo Lafont,^{‡,§} Erik M. Kelder,[‡]
Michiel T. Kreutzer,[‡] and Freek Kapteijn[§]

[†]*Chemical Engineering, Facultad de Ciencias, Universidad Autónoma de Madrid, 28049 Madrid, Spain*, [‡]*NanoStructured Materials, [§]Catalysis Engineering, and [‡]Process and Product Engineering, DelftChemTech, Applied Sciences, Delft University of Technology, 2628 BL Delft, The Netherlands*

Received September 17, 2009

A novel, versatile method is introduced for the fast and continuous preparation of nanoparticles with controlled size, based on the electrostatic spraying of a precursor solution into a reductive-surfactant solution at room temperature. The technique is demonstrated by the production of anisotropic gold nanoparticles and based on the electrostatic aerosol generation of a HAuCl_4 precursor solution followed by the chemical reduction of Au^{3+} to metallic gold (Au^0) by dodecylaminomethanol (DDAM), which is a bifunctional molecule that acts both as a reducing agent and, subsequently, as a stabilizing (capping) agent. The particle size depends on the droplet size in the spray and can be tuned by properly selecting the flow rate, precursor concentration, and applied voltage. In this way, small and uniform quasi-spherical gold nanoparticles of 4.5 nm edge size can be prepared within <1 h and decahedrons of 10–12 nm edge size can be prepared within (only) a few minutes. This synthesis technique opens possibilities for scale-up by numbering-out of the continuous production of nanoparticles with controlled particle size for a wide range of applications.

1. Introduction

The intrinsic properties of metals at nanoscale length, dictated by the size, shape, and crystalline structure of the resulting nanoparticles, are particularly attractive for various technological applications. The development of preparative methodologies for tailoring both particle shape and size has been intensified recently, giving special attention to the preparation of noble metal nanoparticles (viz, Ag, Pt, Pd, and Au).^{1–4}

Liquid-phase synthesis is usually preferred over gas-phase approaches in the preparation of metallic anisotropic nanoparticles.⁵ The participation of a size and shape-conductor molecule—called capping or stabilizing agent—is crucial for this type of synthesis. This molecule

binds on specific facets of the nanocrystal formed in solution. Indeed, it promotes the growth at the “free” crystal facets, which determines the final shape for the grown particle.⁶ The standard protocol for the preparation of anisotropic nanoparticles in an aqueous phase is referred to as seed-mediated growth.^{4,7} It is a multistep method that requires the participation of different chemicals (precursor, several reducing agents, capping agent). The so-called “polyol process” is relevant when organic solvents are used.^{3–5} However, this method requires high temperatures and long-time reactions. The concurrent control of shape, size, and crystal structure in the same liquid-phase preparation still represents a real challenge for this type of material. For instance, anisotropic multiple twinned nanoparticles are attractive candidates for catalytic applications because of the favorable adsorption of small molecules, such as oxygen and hydrogen, on their twin boundaries.^{2,8,9} However, these particles are usually obtained with features that usually limit or exclude their catalytic applications (i.e., relatively large sizes).^{1,10}

*Author to whom correspondence should be addressed. Tel.: +34 914972878. Fax: +34 914973516. E-mail: asun.quintanilla@uam.es.

(1) (a) Wiley, B.; Sun, Y.; Mayers, B.; Xia, Y. *Chem.—Eur. J.* **2005**, *11*, 454. (b) Xu, J.; Li, S.; Weng, J.; Wang, X.; Zhou, Z.; Yang, K.; Liu, M.; Chen, X.; Cui, Q.; Cao, M.; Zhang, Q. *Adv. Funct. Mater.* **2008**, *18*, 277. (c) Seo, D.; Yoo, C. I.; Chung, I. S.; Park, S. M.; Ryu, S.; Song, H. *J. Phys. Chem. C* **2008**, *112*, 2469.

(2) Xiong, Y.; Xia, Y. *Adv. Mater.* **2007**, *19*, 3385.

(3) Zhang, Q.; Xie, J.; Yang, J.; Lee, J. Y. *ACS Nano* **2009**, *3*(1), 139.

(4) Lim, B.; Jiang, M.; Tao, J.; Camargo, P. H. C.; Zhu, Y.; Xia, Y. *Adv. Funct. Mater.* **2009**, *19*, 189.

(5) (a) Tao, A. R.; Habas, S.; Yang, P. *Small* **2008**, *4*, 310. (b) Grzelczak, M.; Perez-Juste, J.; Mulvaney, P.; Liz-Marza, L. M. *Chem. Soc. Rev.* **2008**, *37*, 1783.

(6) (a) Sun, Y.; Mayers, B.; Herricks, T.; Xia, Y. *Nano Lett.* **2003**, *3*, 955. (b) Murphy, C. J. *Science* **2002**, *298*, 2139. (c) Bratlie, K. M.; Lee, H.; Komvopoulos, K.; Yang, P.; Somorjai, G. A. *Nano Lett.* **2007**, *7*, 3097. (d) Zhang, G. H.; Guo, W. L.; Wang, X. K. *Mater. Res. Innovat.* **2007**, *11*, 201.

(7) (a) Busbee, B. D.; Obare, S. O.; Murphy, C. J. *Adv. Mater.* **2003**, *15*, 414. (b) Murphy, C. J. *J. Am. Chem. Soc.* **2004**, *126*, 8648. (c) Murphy, C. J.; Sau, T. K.; Gole, A. M.; Orendorff, C. J.; Gao, J.; Gou, L.; Hunyadi, S. E.; Li, T. *J. Phys. Chem. B* **2005**, *109*, 13857.

(8) Xiong, Y.; McLellan, J. M.; Yin, Y.; Xia, Y. *Angew. Chem., Int. Ed.* **2007**, *46*, 790.

(9) Calvo, F.; Carré, A. *Nanotechnology* **2006**, *17*, 1292.

(10) (a) Berhault, G.; Bausach, M.; Bisson, L.; Becerra, L.; Thomazeau, C.; Uzio, D. *J. Phys. Chem. C* **2007**, *111*, 5915. (b) Wiley, B.; Herricks, T.; Sun, Y.; Xia, Y. *Nano Lett.* **2004**, *4*, 1733.

Conversely, the preparation of metallic nanoparticles can be also performed via the gas phase, relying on the generation of a metallic aerosol. The aerosolization can be obtained, for example, by the electrospraying of a metallic colloidal solution,^{11,12} by spark discharge generation between two metallic electrodes,^{13,14} or by evaporation/condensation of a metallic mesh coupled with an excimer lamp.¹⁵ In the last two cases, small, spherical primary particles (<5 nm) are formed from the mesh or electrode, which agglomerate in an uncontrolled way to clusters of 50–200 nm in size.^{14,15} Electrospraying generates highly charged, self-dispersing droplets, limiting the agglomeration for the resulting particles. Besides, it is also the method that consumes the least energy, when compared to those previously mentioned. This technique has been used for the spray of metallic nanoparticles from colloidal solutions on a substrate¹⁶ or, in the absence of the substrate, for the production of fine powders of small sizes (<10 μm).¹² The solid particles are obtained once the solvent evaporates from the fine droplets generated by electrospraying of the colloid. The size of the particles can be tuned before electrospraying by modification of the metal concentration in the colloid.

In this work, we present a novel method for the preparation of anisotropic gold nanoparticles that combines the advantages of the liquid- and gas-phase approaches. Shape and size can be controlled by the presence of a capping agent in the liquid phase, while small particle sizes, suitable for catalysis applications, can be achieved by the formation of a precursor aerosol. This new technique relies on electrospraying of a metallic precursor solution into liquid solutions containing reductive surfactants. It is a one-step preparation method with reaction times of few minutes that is conducted at room temperature. Continuous production on a larger scale via this process can be eventually performed by multiplexed nozzle systems. Furthermore, an attractive feature is that, apart from the metallic precursor, only one additional chemical compound is required (here, this compound is, namely, dodecylaminomethanol (DDAM), which is a molecule that acts both as a reducing agent and a capping agent). Anisotropic gold nanoparticles are synthesized and stabilized in the liquid phase via the reduction of Au^{3+} , contained in the electrosprayed droplets of HAuCl_4 solutions, to metallic gold (Au^0) via a reductive solution of DDAM. The effects of the principal operating conditions (i.e., flow rate, initial precursor concentration, and applied voltage) on the particle shape and size are studied.

- (11) (a) Lenggoro, I. W.; Xia, B.; Okuyama, K.; Fernandez de la Mora, J. *Langmuir* **2002**, *18*, 4584. (b) Schulz, F.; Franzka, S.; Schmid, G. *Adv. Funct. Mater.* **2002**, *12*, 532. (c) Suh, J.; Han, B.; Okuyama, K.; Choi, M. J. *Colloid Interface Sci.* **2005**, *287*, 135.
- (12) Jaworek, A. *Powder Tech.* **2007**, *176*, 18.
- (13) Byeon, J. H.; Park, J. H.; Hwang, J. J. *Aerosol. Sci.* **2008**, *39*, 888.
- (14) Seipenbusch, M.; Weber, A. P.; Schiel, A.; Kasper, G. *J. Aerosol. Sci.* **2003**, *34*, 1699.
- (15) (a) Deppert, K.; Krinke, T.; Magnusson, M. H.; Malm, J.; Samuelson, L. J. *Aerosol. Sci.* **1998**, *S531*. (b) Nakaso, K.; Shimada, M.; Okuyama, K.; Deppert, K. *J. Aerosol. Sci.* **2002**, *1061*.
- (16) Böttger, P. H. M.; Bi, Z.; Adolph, D.; Dick, K. A.; Karlsson, L. S.; Karlsson, M. N. A.; Wacaser, B. A.; Deppert, K. *Nanotechnology* **2007**, *18*, 105304.

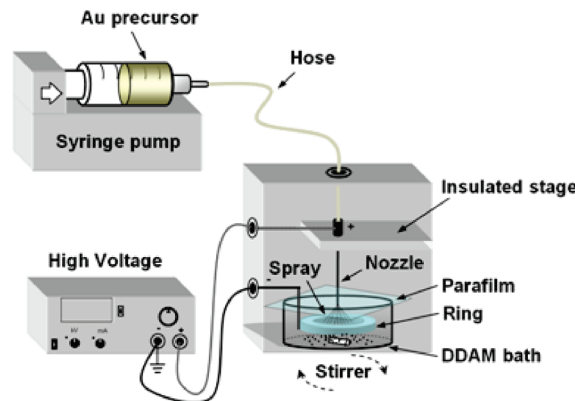
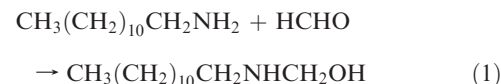


Figure 1. Experimental setup for electrospray in reductive solution.

2. Experimental Section

Precursor solutions for the spraying with concentrations of gold covering 2 orders of magnitude (0.25–24.5 mM) are prepared by dissolving $\text{HAuCl}_4 \cdot 3\text{H}_2\text{O}$ (>99.9%, Aldrich) in isopropanol (>99%, J.T. Baker). Water is not recommended as a solvent, because its electrical conductivity and surface tension are too high and hinder stable electrospraying (ES). The reductive-surfactant solution of DDAM in cyclohexane (>99%, J.T. Baker) is prepared via the reaction of DDA (>99.5%, Fluka) and formaldehyde (FA) (ACS reagent, Sigma–Aldrich) at room temperature.¹⁷ For a typical preparation, 4 mmol of DDA is dissolved in 25 mL of cyclohexane, then 0.16 mol of aqueous FA (37 wt % in water) is added. After vigorous stirring for at least 10 min (the time needed for complete DDA conversion, as proven by GC-MS and ^{13}C NMR),¹⁷ the cyclohexane phase, which now contains DDAM, is separated from the aqueous phase with the residual FA:



According to the reaction stoichiometry, a solution of 0.16 M of DDAM in cyclohexane is obtained.¹⁷

In each experiment, a 10-mL glass syringe (Fortuna Optima) is filled with 5 mL of the precursor solution. The syringe is placed in a syringe pump (KD Scientific, Model 100 series), which is used to inject the precursor solution with a constant flow rate through an electrified nozzle with a flat rim and straight cutoff (stainless steel, 0.25 mm inner diameter (id), EFD Ultra). Typically, flow rates of 0.5 and 2 mL/h are selected. The voltage between the nozzle and the counter electrode is set at ~4.5 or 9.5 kV, to generate the precursor aerosol. A counter electrode ring (soldering alloy-Sn:Pb 60:40) is placed in a beaker containing 21 mL of 0.16 M DDAM solution. A simplified scheme of the experimental setup for electrospraying is shown in Figure 1, and the operating conditions of the experiments performed are reported in Table 1. The experiments are further labeled according to the following notation: R-(precursor concentration)-(flow rate)-(voltage value). The experimentation time varies from 3 min to 50 min, depending on the flow rate and the precursor concentration employed, to obtain the same final gold concentration in the colloid (i.e., ~0.10 mM).

- (17) Chen, Y.; Wang, X. *Mater. Lett.* **2008**, *62*, 2215.

Table 1. Gold Nanoparticles Prepared by Electrospraying under Different Experimental Conditions^a

sample	$C_{\text{precursor}}$ (mM)	$Q_{\text{precursor}}$ (mL/h)	$F_{\text{precursor}}$ (mg/h)	$t_{\text{experiment}}$ (min)	V_{DDAM} (mL)	V (kV)	spraying mode	d_p (nm)	shape
R-4-0.5-9	4	0.5	1.0	48	21	9.0	multi-jet	5.3 ± 1.4	quasi-spherical
R-2-2-2-9.5	2.2	2	0.8	12	21	9.5	multi-jet	8.0 ± 2.6	quasi-spherical
R-4-2-9.5	4	2	1.6	12	21	9.5	multi-jet	12.4 ± 2.8	branched
R-24-2-9.5a	24	2	9.5	3	21	9.5	multi-jet	5 and 20	
R-24-2-9.5b ^b								5 ± 1	spherical
R-24-2-9.5c ^c								9 and 21	icosahedral and decahedral
R-4-2-4.5	4	2	1.6	12	21	4.5	cone-jet	8.8 ± 2.4	decahedral
R-27.7-2-0	27.7	2	10.8	3	21	0	dripping	15.9 ± 3.5	hexagonal

^aThe final gold concentration in the resulting colloids is always ~0.10 mM. ^b Sample R-24-2-9.5a measured after centrifugation to remove the bigger particles. ^c Sample R-24-2-9.5a measured two weeks after preparation.

Before starting the reaction, the tubing (chemically resistant rubber hose with an outer diameter of $1/16$ in., Watson Marlow) that connects the syringe to the nozzle is completely filled with the precursor solution. A selected voltage then is applied between the nozzle and the counter electrode, and stirring of the reductive solution is started. After these steps, the syringe pump is switched on and the onset of ES occurs immediately, with the emission of charged droplets attracted toward the reductive-surfactant solution. The shape of the droplets is influenced by the form of the meniscus and the mode of spraying for a fixed flow rate. In our experiments, the spherical shape of the pendant liquid droplet is progressively deformed to a conical shape for low voltages (≤ 5 kV). From the tip of this conical meniscus, a thin jet is ejected. (For this reason, this mode is known as “cone-jet”.) For higher voltages (≥ 9 kV), at a fixed flow rate, more jets are introduced, distributing the initial flow among different cone-jets. This mode is also known as “multi-jet”.¹⁸

The crystal structure and the size of the particles were further investigated by a Philips Model CM30T transmission electron microscopy (TEM) system operated at 300 kV. The total gold content in the precursor and colloidal solutions was determined by a graphite furnace atomic absorption spectroscopy (AAS) (Perkin–Elmer, Model 4100ZL). The plasmon resonance of the colloids was measured with a UV–vis spectrophotometer (UNICAM Model UV 500).

Electrospraying Theory. To aid the discussion, some basic elements of the electrospraying technique are given here in relation to the experimental conditions applied.

The size of the droplets in the electrospray is governed by a combination of parameters. Hartman et al.¹⁹ proposed the following expressions for the calculation of the droplet size in the “cone-jet” mode:

$$d_{d,v} = c \left(\frac{\rho \epsilon_0 Q^4}{I^2} \right)^{1/6} \quad (\text{for varicose break-up}) \quad (2)$$

where monodispersed droplets are formed, because of minimal perturbation of the lateral electrical forces, and

$$d_{d,w} = \left[0.8 \left(\frac{288 \epsilon_0 \gamma Q^2}{I^2} \right) \right]^{1/3} \quad (\text{for break-up by whipping motions}) \quad (3)$$

(18) Cloupeau, M.; Prunet-Foch, B. *J. Aerosol Sci.* **1994**, *25*, 1021.
 (19) (a) Hartman, R.P. A.; Brunner, D. J.; Camelot, D. M. A.; Marijnissen, J. C. M.; Scarlett, B. *J. Aerosol Sci.* **1999**, *30*, 823.
 (b) Hartman, R.P. A.; Brunner, D. J.; Camelot, D. M. A.; Marijnissen, J. C. M.; Scarlett, B. *J. Aerosol Sci.* **2000**, *31*, 65.

Table 2. Current Intensity and Maximum Droplet Sizes Expected in the “Cone-Jet” Mode for Pure Isopropanol Calculated via the Expressions Proposed by Hartman et al.,¹⁹ as a Function of the Typical Flow Rates Used in This Work

Q_L (mL/h)	I (nA)	$d_{d,v}$ (μm)	$d_{d,w}$ (μm)
0.5	8.4	11.5	23.0
2	16.8	23.1	36.5

where the droplets generally lose their monodispersity because of enhanced lateral electrical forces that cause the liquid jet to whip and break irregularly.

In eqs 2 and 3, ρ is the density of the liquid, c a numerical constant close to 2, ϵ_0 the permittivity of free space, γ the surface tension, and I the current that flows through the liquid cone, which is approximately given by

$$I \approx 2(\gamma \kappa Q)^{1/2} \quad (4)$$

where Q is the flow rate and κ is the electrical conductivity of the liquid.

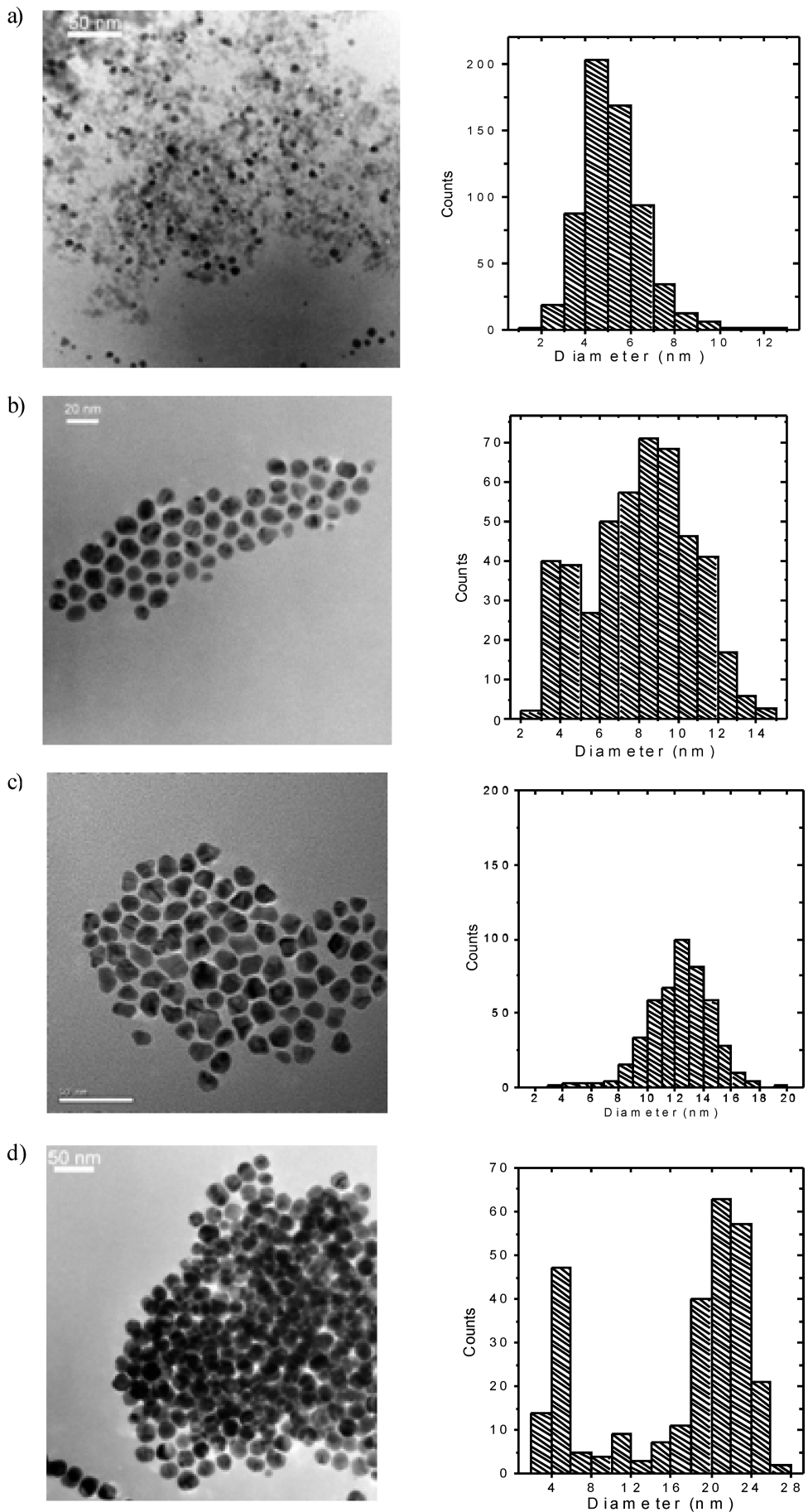
The flow rate Q is the factor that dominates the droplet size. Also, the surface tension γ and the electrical conductivity κ are important, because they are contained in I . The voltage does not appear in eqs 2–4 because electro-spray is a field-driven process.

These considerations apply only to the “cone-jet” mode. For “multi-jet” mode, a complete description in terms of “scaling laws” (eqs 2–4) does not exist at the moment.

Considering the ES of pure isopropanol, whose electrical conductivity ($\kappa = 5.8 \times 10^{-6}$ S/m) is lower than the value expected for the gold precursor solutions, the maximum droplet size that can be obtained at the typical flow rates used (0.5 and 2 mL/h) has been calculated according to eqs 2 and 4 (see Table 2). The isopropanol physical properties (at 25 °C) that have been used for the calculation are given as follows: $\rho = 790 \text{ kg/m}^3$, $\gamma = 22 \times 10^{-3} \text{ N/m}$, and $\mu = 1.96 \times 10^{-3} \text{ Pa s}$. For pure isopropanol, the jet break-up mechanism is likely to occur via varicose instabilities, because it results in $d_{d,v} < d_{d,w}$ for both flow rates used. Accordingly, in the “cone-jet” mode, droplet sizes of $< 23 \mu\text{m}$ and a certain monodispersity for the aerosol produced are expected.

In “multi-jet” mode, the droplet emission frequency is much higher than that in “cone-jet” mode, together with the electrical forces involved and, consequently, the current flowing between the cone and the counter electrode. The thin jets formed at the rim of the nozzle disperse into a fine, highly charged aerosol mist via *whipping* motions.²⁰ In this scenario, the occurrence of electrical discharges in the surrounding atmosphere also should be considered, which can completely destabilize the droplet production process and easily lead to a loss of monodispersity.

(20) Jaworek, A.; Krupa, A. *J. Aerosol Sci.* **1999**, *30*, 873.



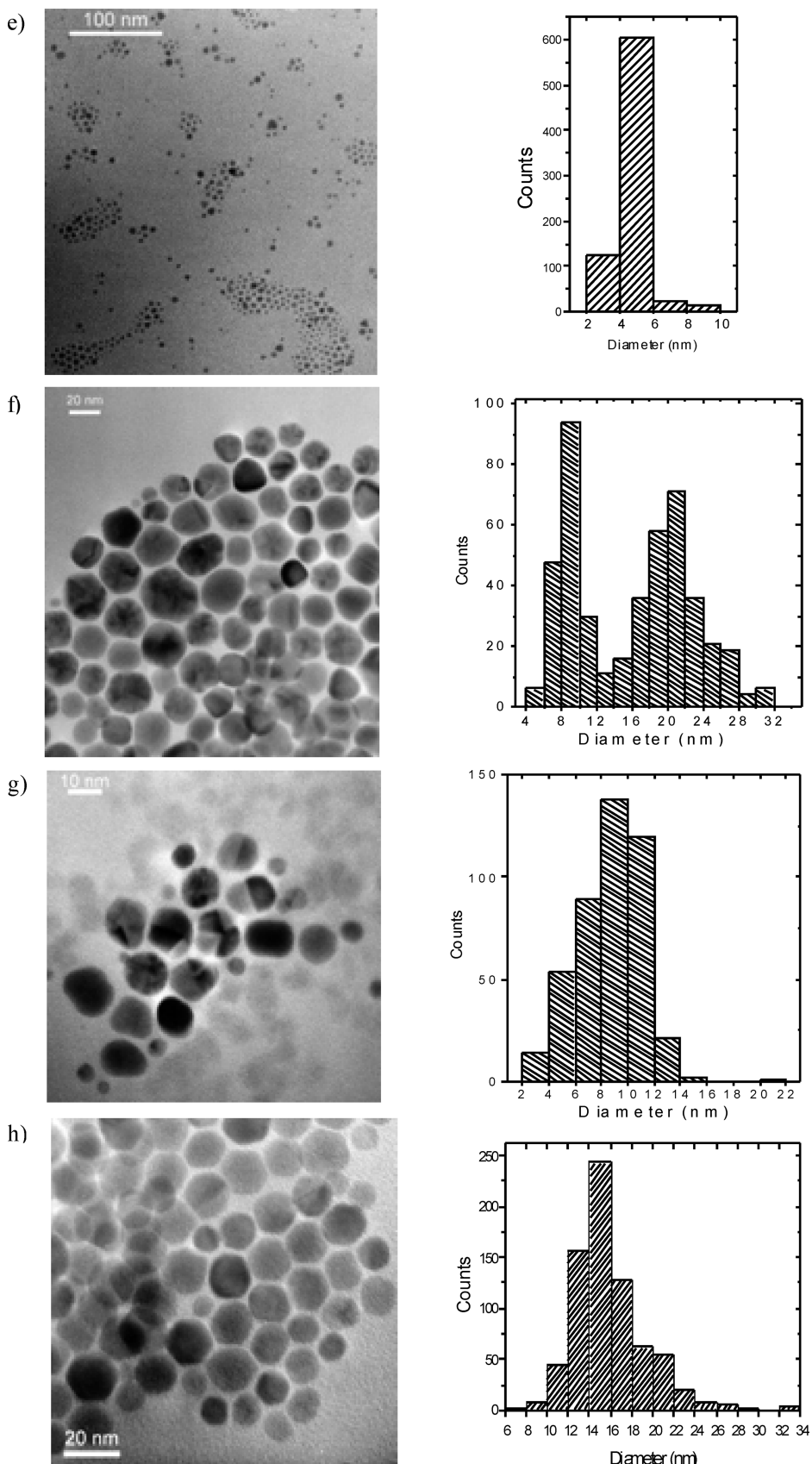


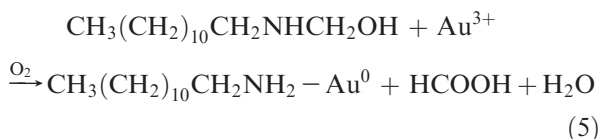
Figure 2. TEM micrographs and corresponding particle size distributions of the samples related to experiments (a) R-4-0.5.9, (b) R-2.2-2-9.5, (c) R-4-2-9.5, (d) R-24-2-9.5a, (e) R-24-2-9.5b, (f) R-24-2-9.5c, (g) R-4-2-4.5, and (h) R-27.7-2-0 (from Table 1; note that sample R-24-2-9.5c was measured 2 weeks after preparation).

Therefore, the “multi-jet” mode can also result in a nonuniform droplet production, where, sometimes, irregular liquid

fragments are emitted. Hence, a larger particle size can be eventually obtained under such circumstances.

3. Results and Discussion

During electrospraying, the droplets containing the Au^{3+} anions are driven into the stirred DDAM solution. The reductive functional group in DDAM ($-\text{NHCH}_2\text{OH}$) is oxidized to $-\text{NHCOOH}$ by Au^{3+} , which, at the same time, is reduced to Au^0 . The $-\text{NHCOOH}$ group is not stable and decomposes to $-\text{NH}_2$ and formic acid. Consequently, DDA is released while being readily adsorbed and assembled on the nanoparticle surface. The entire process is then responsible for the change of color of the solution, which turned pink, and the formation of the stabilized colloid:



The protection of the nanoparticles in the colloidal solution by DDA was demonstrated by Fourier transform infrared (FT-IR) analyses.¹⁷

It is worthwhile to mention that all the resulting colloidal solutions had a pink color, in contrast to the characteristic red color displayed by spherical gold nanoparticles. The plasmon resonance is exhibited at 524 nm, which is within the range attributed to small gold nanoparticles ($< 30 \text{ nm}$).²¹

The average particle sizes measured by TEM on the same day of the synthesis are reported in Table 1. For those particles with a quasi-spherical shape, the size represents the diameter, while for the specific shape (decahedrons and short rods), it refers to the diagonal. The particle morphology and their relative size distribution are shown in Figure 2.

The size distribution is quite broad (see Table 1 and Figure 2). This heterogeneity in size is expected when a burst nucleation within an extremely short period of time, followed by slow growth, does not occur.²² In our system, nucleation proceeds simultaneously to the particle formation, because of the continuous electrospray of Au^{3+} species in the stirred reductive solution. Then, “seed-mediated” growth is likely to happen. The particle size distribution in this case can be narrowed by a subsequent digestive ripening of the nanoparticles,²³ and, when there is a clear bimodal distribution, as in experiment R-24-2-9.5a, centrifugation can be a tool to separate both sizes (experiment R-24-2-9.5b).

The experimental parameter settings (i.e., flow rate, gold concentration in the precursor solution, and applied voltage for the atomization of the precursor) determine the particle size. More specifically, it depends on the droplet size, the concentration of Au^{3+} ,

per droplet, and the emission frequency of the generated droplets.

Influence of the Flow Rate. A lower flow rate favors smaller particle sizes (cf. experiments R-4-0.5-9 and R-4-2-9.5 in Table 1) at the same precursor concentration and similar applied voltage in the “multi-jet” mode.

The lower the flow rate, the smaller the droplet size in the generated aerosol (see eqs 2 and 3 for the “cone-jet” mode) and the lower the feed rate of the gold species into the reductive-surfactant solution. Simultaneously, the concentration of gold in the droplet is expected to increase, because, for smaller droplets, the solvent evaporates faster. The first aspect (droplet size) seems to have a stronger influence on the particle size. The resulting particle sizes— $5.3 \pm 1.4 \text{ nm}$ at 0.5 mL/h (R-4-0.5-9) and $12.4 \pm 2.8 \text{ nm}$ at 2 mL/h (R-4-2-9.5)—indicate that more than one nanoparticle is likely produced from one single droplet a few micrometers in size.

Influence of the Gold Concentration in the Precursor Solution. A higher initial concentration of Au^{3+} in the precursor solution, at a given flow rate and applied voltage in the “multi-jet” mode, favors larger particle sizes (experiments R-2.2-2-9.5, R-4-2-9.5, and R-24-2-9.5 in Table 1), disregarding, in the last case, the formation of particles with an average size of 5 nm. On one hand, a higher concentration of Au^{3+} implies a higher electrical conductivity of the solution (κ) and, consequently, the formation of smaller droplets, as suggested by eqs 2–4. Generally, we can expect competition between the nucleation–growth process of the gold particles due to the continuous supply of species (i.e., the more concentrated the emitted droplets, the bigger the amount of precursor readily available for particle formation and growth) and the moderate decrease of the average droplet size by increasing the entire solution conductivity.

The evolution of the particle size with the gold precursor concentration at a fixed flow rate of 2 mL/h and applied voltage of 9.5 kV is presented in Figure 3. The influence of the gold concentration is more pronounced at values of $< 5 \text{ mM}$ in the precursor solution.

In addition, the particle size can be reduced, for a given concentration, by further decreasing the droplet size, i.e., using lower flow rates.

Influence of the Applied Voltage. Increasing the voltage causes the introduction of “multi-jet” operation; however, this can also enhance the presence of some liquid fragments for the electrosprayed precursor, which result from irregular breakup of the thin jets under conditions of electrical discharge. This is a possible explanation for the outcome of experiment R-4-2-9.5, which was performed at 9.5 kV . Indeed, larger particle sizes are obtained than in experiment R-4-2-4.5 conducted at 4.5 kV (i.e., 12.4 nm vs 8.8 nm , respectively, both at the same flow rate, precursor concentration, and reaction time; see Table 2).

Furthermore, a reference experiment was conducted without applying any voltage, by dripping the gold precursor solution into the reductive-surfactant solution. The experiment labeled R-27.7-2-0 in Table 1 and the related TEM image reported in Figure 2g show that the

(21) (a) Sakura, T.; Nagasaki, Y. *Colloid Polym. Sci.* **2007**, *285*, 1407.
 (b) Yang, Y.; Matsubara, S.; Nogami, M.; Shi, J. *Mater. Sci. Eng., B* **2007**, *140*, 172.
 (22) Park, J.; Joo, J.; Kwon, S. G.; Jang, Y.; Hyeon, T. *Angew. Chem., Int. Ed.* **2007**, *46*, 4630.
 (23) Zhang, Q. B.; Xie, J. P.; Lee, J. Y.; Zhang, J. X.; Boothroyd, C. *Small* **2008**, *4*, 1067.

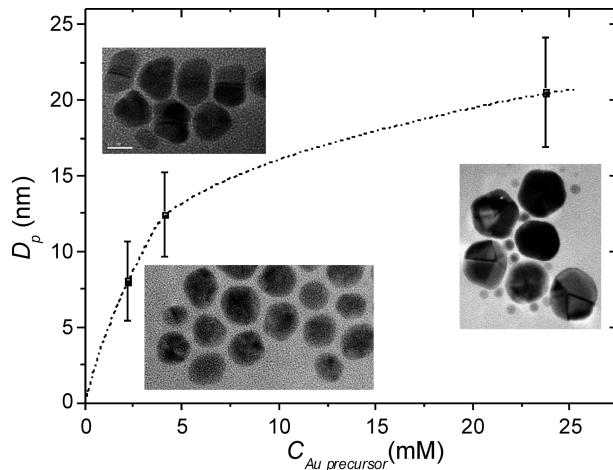


Figure 3. Dependence of the particle size on the sprayed gold precursor solution. (Flow rate = 2 mL/h and applied voltage = 9.5 kV.) The insets show TEM images of the samples synthesized under the corresponding conditions (experiments R-2.2-2-9.5, R-4-2-9.5, and R-24-2-9.5a).

particle size is hardly affected, at least when compared with experiment R-24-2-9.5. The main difference comes from the particle morphology, exhibiting single-crystal instead of polycrystalline shapes.

We observed that the kinetics of the nanoparticle synthesis was directly affected by the use of the voltage. Without any voltage, the reaction kinetics was considerably slow, and it took several minutes before the reductive solution started to change gradually in color and reached the final hue after complete dripping of the precursor. On the other hand, experiments with ES showed a steady change of color of the reductive solution, which normally had reached its final hue directly at the end of the experiment.

Taking into account the influence of the experimental parameters, it can be concluded that (i) the charged droplets created with ES are mainly responsible for the observed nanoparticle polycrystallinity and (ii) the size of the produced particles is governed by the droplet size, gold concentration, and stability of the ES process.

Interestingly, only polyhedral particles were synthesized according to the TEM micrographs (see Figure 2). Depending on the operating conditions, they are geometrical projections of irregular shapes (experiments R-4-0.5-0, R-2.2-2-9.5, and R-4-2-9.5; see Figures 2a, 2b, and 2c, respectively) or decahedrons and icosahedrons (experiments R-24-2-9.5a and R-4-2-4.5; see Figures 2d and 2e, respectively). The formation of mixtures of nanoparticles with different morphologies usually occurs when there is a heterogeneous reaction environment for each particle.²³

The lowest flow rate (0.5 mL/h, experiment R-4-0.5-9) results in small, uniform nanoparticles (5.3 ± 1.4 nm) with quasi-spherical shapes (see Figure 2a) with a 4.5 nm edge size. An increase in flow rate, maintaining the same precursor concentration (experiment R-4-2-9.5), results in a change in the morphology of the particles and their size. Branched nanoparticles are then produced (see Figure 2b). The formation of these anisotropic nanoparticles is caused by a preferential addition of Au atoms at the high-energy edge sites.¹⁰ The Au^0 atoms are preferentially added to the energetically most unstable atoms of the

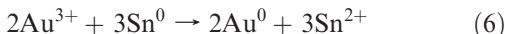
particle. At a high (gold) precursor concentration (experiment R-24-2-9.5a), well-defined polycrystalline nanoparticles (mainly icosahedrons and some decahedrons with 10 and 12 nm edge sizes, respectively) are obtained (see Figure 2c). Their average size is 20.5 ± 3.6 nm. It is worthwhile to mention that also short rods (20 nm in length) can be detected in the micrograph. The presence of the rods suggests that the decahedrons are polycrystalline with multiple-twinned structures, as earlier reported in the literature.⁶ The small, spherical, single-crystal nanoparticles of 5 nm—likely the most recently formed—were not considered, although their concentration in the colloid was high enough to show a bimodal distribution. These small particles could be separated via centrifugation (experiment R-24-2-9.5b, Figure 2d). This bimodal distribution is attributed to the different aging time of the particles in the solution, as a consequence of the semi-batch operation, and/or to the possibility that not all the droplets are uniformly charged at this high gold precursor concentration, resulting in a fraction of single-crystal nanoparticles.

The evolution of the nanoparticle shape with the precursor concentration is represented in Figure 3. The concentration of gold in the emitted droplet is important for the particle shape. The more concentrated the emitted droplets, the larger the amount of precursor readily available for particle formation and growth. Accordingly, more regular nanoparticles are obtained.

Stability of the Nanoparticles. The “as-prepared” colloidal solutions can contain up to 25% less gold than expected, according to the mass feed flow rate and the reaction time. For instance, for experiment R-4-2-9.5, the measured concentration of total gold, as determined by AAS, is 0.06 mM, whereas the expected one is 0.08 mM. The deposition of gold on the counter electrode can occur by some interaction between the gold and the metals of the electrode (soldering alloy Sn:Pb 60:40), as indicated by the slight darkening of the counter electrode after reaction.

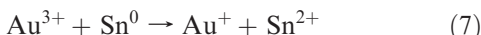
Considering the standard reduction potentials of the metals, gold has a higher potential ($E^\circ = 1.498$ V) than tin

($E^\circ = -0.1375$ V), therefore, gold can be spontaneously reduced by the tin electrode via electroless deposition:



This phenomenon can be avoided by using an inert or coated electrode.

Also, the partial reduction of gold can eventually occur at the surface of the electrode:



Au^+ in solution undergoes disproportion, according to the reaction



because $E^\circ(\text{Au}^+/\text{Au}^0) > E^\circ(\text{Au}^{3+}/\text{Au}^0)$. However, Au^+ exists only as a stable form in solution as a complex ion (i.e., $[\text{AuCl}_2]^-$),²⁴ so eq 8 is less expected.

Two weeks after preparation, some particles in solution precipitated at the bottom of the beaker and the total amount of gold in the solution was reduced by 80%, although the particle size did not change (R-24-2-9.5c, Figure 2e). This instability may be due to a change in the ionic strength of the colloidal solution caused by the presence of isopropanol. Indeed, gold nanoparticles prepared by the same precursor ($\text{HAuCl}_4 \cdot 3\text{H}_2\text{O}$) and reductive solution (DDAM in cyclohexane), following the same methodology described by Chen and Wang,¹⁷ which is based on a novel phase-transfer preparation method, are stable for months. This instability can be avoided by washing the excess of reducing agent (DDAM) of the “as-prepared” colloid with ethanol and subsequent redispersion of the nanoparticles in a nonpolar solvent.

The method of electrospraying into a reductive solution allows a fast one-step synthesis of anisotropic gold nanoparticles at room temperature with an appropriate size for catalytic applications (5–12 nm edge size). The experimentation time varies from 3 min to 50 min, with a final gold colloid concentration of ~0.10 mM. The use of higher gold precursor concentrations can lead to larger particle sizes, because of their easier growth when more precursor is directly available in the electrosprayed droplets, unless lower flow rates (i.e., smaller droplets) are used to compensate for the increase. Ultimately, the droplet size and gold concentration determine the resulting particle size.

The continuous production of the polycrystalline anisotropic gold nanoparticles with controlled size on a larger

scale by electrospraying can be envisioned by outscaling via multiplexed nozzle systems. The current operation is performed semibatch-wise, resulting in increasing concentrations of particles in the reductive solution and a broad age distribution. If particle growth occurs by agglomeration or Ostwald ripening, one may consider even electrospraying into a flowing film solution, resulting in a real continuous operation with a more uniform age distribution.

The use of other bifunctional components, acting as both a reducing agent and a capping agent, is obvious.²⁵ Here, DDAM was used to avoid contamination of the gold catalytic performance by capping agents that are too strongly binding, based on sulfur or phosphorus.

Although the technique has been demonstrated for the production of gold nanoparticles for catalytic application, in principle, it can be developed for the production of any type of metallic nanoparticles with applications in other fields (e.g., batteries, hydrogen storage, and optoelectronics).

4. Conclusions

A versatile method for the fast preparation (in one step) of anisotropic gold nanoparticles in organic solvents at room temperature is reported, which offers an outlook for larger-scale and continuous production of metallic nanoparticles in general. It is based on electrospraying into a reductive-surfactant solution that contains a bifunctional component, acting both as a reducing agent and as a capping agent. In this study, anisotropic gold nanoparticles with appropriate sizes for catalysis applications (5–12 nm edge size) have been successfully produced. The droplet size of the precursor solution in the spray can be tuned by selecting the flow rate, precursor concentration, and applied voltage, which are the major parameters that determine the particle size. Quasi-spherical nanoparticles with a 4.5 nm edge size can be obtained within 50 min, while, for the same productivity, decahedrons with a 10–12 nm edge size are obtained within 3 min; this shorter preparation time results in a larger particle size, in a wider size distribution and a larger heterogeneity in shapes. The high flexibility of this method, combined with the easy operation and the reduced costs of the equipment, makes this process a good candidate for quantitative production of nanoparticles in general (i.e., scale-up by multiplexed nozzle systems).

Acknowledgment. The authors acknowledge the Delft Center for Sustainable Industrial Processes (DC-SIP) for the financial support.

(24) Silvestroni, P. *Fondamenti di Chimica*; Casa Editrice Ambrosiana: Milan, Italy, 1997. (ISBN: 9788840809984.)

(25) Witte, P. T. International Patent WO/2009/096783, 2009.